ORIGINAL RESEARCH

Detection and Characterization of Intracranial Aneurysms with 16-Channel Multidetector Row CT Angiography: A Prospective Comparison of Volume-Rendered Images and Digital Subtraction Angiography

D.Y. Yoon
K.J. Lim
C.S. Choi
B.M. Cho
S.M. Oh
S.K. Chang

BACKGROUND AND PURPOSE: The aim of our study was to compare multidetector row CT angiography (MDCTA) with digital subtraction angiography (DSA) in the detection and characterization of intracranial aneurysms.

MATERIALS AND METHODS: In our blinded prospective study, 85 patients with suspected intracranial aneurysm (47 women, 38 men; age range, 19–83 years) underwent both 16-channel MDCTA and DSA. The MDCT angiograms were interpreted for the presence, location, size, ratio of the neck to the dome (N/D ratio), and lobularity of the aneurysms and relationship of the aneurysm with the adjacent arterial branches, by using volume-rendering techniques. MDCTA and DSA images (reference standard) were interpreted by 2 independent readers, and the results were compared.

RESULTS: A total of 93 aneurysms were detected at DSA in 71 patients, whereas no aneurysms were detected in 14 patients. Compared with DSA, the overall sensitivity, specificity, and accuracy of MDCTA on a per-aneurysm basis were 92.5%, 93.3%, and 92.6%, respectively, for both independent readers. For aneurysms of <3 mm, however, MDCTA had a sensitivity of 74.1% for reader 1 and 77.8% for reader 2. There was excellent agreement between readers in the detection of aneurysms ($\kappa = 0.822$). In addition, MDCTA was also accurate in determining N/D ratio of aneurysms, aneurysm lobularity, and adjacent arterial branches.

CONCLUSION: MDCTA is accurate in the detection and characterization of intracranial aneurysms and can be used as a reliable alternative imaging technique to DSA in selected cases.

Digital subtraction angiography (DSA) has been the standard of reference for the detection and characterization of intracranial aneurysms.[1] It has several disadvantages, however, including the high skill level of performing the procedure and relatively high cost. The invasive nature of DSA is an additional disadvantage, carrying a low but significant 1% complication risk and a 0.07%–1% rate of persistent neurologic deficit.[2-3]

There has, therefore, been increasing interest in the use of noninvasive alternatives for accurate depiction of intracranial aneurysms.[4-5] When compared with DSA, CT angiography (CTA) is a noninvasive imaging technique that does not require arterial puncture or catheter manipulation. It can be easily performed immediately after the initial nonenhanced CT with a single bolus of intravenous contrast medium and allows rapid diagnosis and treatment planning in the acute setting. Furthermore, CTA data can be viewed from almost unlimited projections, facilitating aneurysm detection and characterization.[6-7]

Results of numerous studies have suggested that CTA has high sensitivity and specificity for the detection of intracranial aneurysms.[8-10] However, previous studies of CTA by using single-detector row CT scanners have shown limited diagnostic accuracy in the detection of aneurysms of <3 mm.[11-14] The recent introduction of multidetector row CT (MDCT) can overcome these limitations, offering volumetric acquisition with considerable improvement in the quality and spatial resolution.[15]

The purpose of this prospective study was to compare 16-channel multidetector row CTA (MDCTA) with DSA in the detection and characterization of intracranial aneurysms.

Materials and Methods

Patient Population and Study Design

Between December 2003 and June 2005, 121 consecutive patients with suspected intracranial aneurysms were referred to our institution. The patients were scheduled to undergo conventional DSA and prospectively scheduled to undergo comparative MDCTA. Of them, 27 patients who had undergone prior surgical clipping or endovascular coiling for their intracranial aneurysm were excluded from the study because we believed that postoperative follow-up with MDCTA is a different issue. Another 9 patients who did not undergo DSA because of rapid clinical deterioration were also excluded from our study. There was no patient with contraindication to intravenously administered iodinated contrast material in this series. Thus, our study population consisted of 85 patients; this group included 38 men and 47 women (mean age, 49.6 years ± 14.2; range, 19–83 years).

Patients were selected by the referring physicians for DSA on the basis of clinical or radiologic findings, including presentation with acute subarachnoid hemorrhage confirmed by nonenhanced CT or lumbar puncture ($n = 75$); symptoms and signs suggestive of aneurysm, such as headache or cranial neuropathy ($n = 6$); or a previous

Received October 16, 2005; accepted after revision January 25, 2006.

From the Departments of Radiology (D.Y.Y., K.J.L., C.S.C., S.K.C.) and Neurosurgery (B.M.C., S.M.O.), Hallym University College of Medicine, Seoul, South Korea.

Please address correspondence to Dae Young Yoon, MD, Department of Radiology, Kangdong Seong-Sim Hospital, Hallym University College of Medicine, 445 Gil-dong Kangdong-Gu, Seoul, 134-701, South Korea; e-mail: evee0914@chollian.net

routine CT scan or MR angiogram suggesting the presence of an intracranial aneurysm ($n = 4$).

All patients in the series underwent MDCTA before DSA, with the longest interval between the 2 examinations being 3 days (mean interval between examinations, 13.7 hours ± 16.9). Fifty patients underwent MDCTA and DSA on the same day, with MDCTA performed first and DSA performed 1–2 hours later. In all cases of negative findings on DSA, a second DSA was performed 7–10 days later to ensure the absence of aneurysm. The study protocol was approved by the institutional review board, and informed consent was obtained from all patients or their legal representatives.

MDCTA Protocol

All MDCTA examinations were performed with a 16-channel MDCT scanner (MX8000 Infinite Detector Technology, Philips Medical Systems, Hifa, Israel). After obtaining a lateral scanogram (120 kV, 100 mAs), we planned the scanning range in a caudocranial direction from the level of the foramen magnum through a point 1 cm above the level of the lateral ventricles, including the whole posterior circulation and pericallosal arteries (mean coverage, 70 mm; range, 65–75 mm).

For optimal intraluminal contrast enhancement, the delay time between the start of contrast material administration and the start of scanning was determined for each patient individually by using a bolus-tracking technique (MX8000 Infinite Detector Technology, Philips Medical Systems). For this purpose, a single nonenhanced low-dose scan (20 mAs) at the level of the distal common carotid artery was obtained first. On the basis of this transverse image, a region of interest with an area of 3–5 mm^2 was set in the lumen of the distal common carotid artery. This region of interest served as a reference for the following dynamic measurements of contrast enhancement. Subsequently, a total of 80–100 mL of iohexol (Omnipaque 300, Amersham Health, Cork, Ireland), a low-osmolar iodinated contrast material, was administered through an 18- or 20-gauge needle positioned in a peripheral vein. The contrast medium was administered with a power injector (CT9000ADV, Liebel-Flarsheim, Cincinnati, Ohio) at a rate of 3–4 mL/s. At 10 seconds after the start of contrast material administration, repetitive low-dose monitoring scans (120 kV, 20 mAs, 0.5-second scanning time, 1-second interscan delay) were obtained. When the Hounsfield units in the preset lumen of the distal common carotid artery rose by 100, the MDCT scanning was triggered automatically 3 seconds later.

Parameters for the CT angiographic acquisition were 1-mm section thickness, 6-mm table feed per rotation, 0.5-second gantry rotation time, pitch of 6, 120 kV, and 200–280 mA, 512 × 512 matrix, and 20-cm FOV. MDCTA was performed in all patients without any technical failures or complications during scanning.

3D Reconstruction

The volumetric data so obtained were transferred to a workstation (Rapidia 3D; Infinitt, Seoul, Korea) for further processing. Transverse sections were reconstructed with a section width of 0.5 mm. MDCTA images were processed from the obtained source images by using 2 different methods: 1) volume-rendered technique (VRT) algorithm (in all cases); 2)VRT images after automatic segmentation of a precontrast scan dataset (ie, any overlapping bony structures, calcification, and surgical materials) (in 40 cases). The display of only the contrast-enhanced vascular lumen was possible by using the commercially available software (Rapidia 3D) installed on the workstation. Images were then pictured at 15-degree intervals covering 180° in both cranial-to-caudal and left-to-right projections. The time needed for these reconstructions was 6–8 minutes. The total examination time did not exceed 10 minutes, including VRT images after automatic segmentation. All standardized reconstructions were completed by experienced technicians. The transverse source images and the standardized VRT images (including VRT images with automatic segmentation) were transferred in a separate folder on the workstation.

DSA

All DSA was performed transfemorally with 5F catheters by using a DSA unit (Integris Allura, Philips Medical Systems, Best, the Netherlands) with an image intensifier matrix of 1024 × 1024 pixels. DSA was performed with bilateral selective internal carotid artery injections and either unilateral or bilateral vertebral artery injections, as necessary. Six to 9 mL of nonionic contrast medium (320 mg of iodine per milliliter of iodixanol, Visipaque 320, Amersham Health) was used for each injection at a rate of 4–7 mL/s by using a power injector (Angiomat Illumena, Liebel-Flarsheim). Standard anteroposterior and lateral projections were routinely acquired for carotid and vertebral injections. Additional selected oblique projections were obtained to clarify aneurysm anatomy at the discretion of the angiographer. All acquired DSA images were converted to internationally compatible DICOM files, and then the converted files were transferred to our server through PACS.

Interpretation and Analysis

All MDCTA and DSA images were independently evaluated on the workstations by 2 radiologists, who had 10 (D.Y.Y.) and 3 (K.J.L.) years of experience in CT vascular imaging and angiography. The MDCTA and DSA images were presented in an anonymous random fashion. Each examination was allocated a study number that was known only to the study coordinator. Both readers were blinded to the assessments of the other technique or of the other investigator but knew that the patients were suspected of having intracranial aneurysm.

The reconstructed transverse CT images (source data) and the VRT images were available for both readers on the workstation. For image analysis of the standardized VRT images and source data, a cine mode was available at the workstation for rapid interactive interpretation. Both readers had then the ability of rotating the standardized VRT images to obtain additional oblique projections for better demonstration of the neck of the aneurysm, if considered necessary. DSA images were analyzed separately from MDCTA images; anonymous DSA images were given in random order to the readers 8 weeks after each reader completed the analysis of MDCTA images.

Readers had to refer to specific parameters under the protocol, which included 1) the presence of an aneurysm or aneurysms and the location; 2) the degree of confidence; 3) the size of dome and neck, the ratio of the neck to the dome (N/D ratio), and the lobularity of the aneurysm, as well as the relationship of the aneurysm with the adjacent arterial branches. In addition to diagnostic yield, both readers assessed image quality of MDCTA images with a 3-point scale as follows: 1, excellent; 2, adequate for diagnosis; and 3, inadequate for diagnosis. Grade 1 indicated excellent image quality, which meant that all clinically relevant diagnostic information could be obtained with excellent differentiation of arterial vasculature from background tissue. Grade 2 indicated good image quality, which meant that all clinically relevant diagnostic information could be obtained. Grade 3 indicated nondiagnostic image quality, which meant that diagnostic

Fig 1. A 72-year-old woman with subarachnoid hemorrhage.

A and *B*, Volume-rendered MDCTA images obtained with right anterior oblique (*A*) and lateral (*B*) projections demonstrate a bilobed aneurysm at the bifurcation of the right internal carotid artery (*arrow*). There are also 2 small aneurysms at the posterior communicating artery (*long arrow*) and the anterior choroidal artery (*arrowhead*). The anterior choroidal artery aneurysm was missed by reader 2 at initial interpretation.

C, The same aneurysms (*arrows* and an *arrowhead*) are also depicted on the lateral projection DSA image of the right internal carotid artery.

information could not be obtained because of blurring of the arterial segment or inadequate vessel enhancement.

The presence of aneurysm was assessed by using a 5-point scale of observer's confidence: 1, definitely not present; 2, probably not present, 3, equivocal; 4, probably present; and 5, definitely present. For analysis purposes, the aneurysm location was recorded with the following codes: 1, M1 segment of middle cerebral artery (MCA); 2, MCA bifurcation; 3, distal MCA; 4, A1 segment of anterior cerebral artery (ACA); 5, anterior communicating artery; 6, distal ACA; 7, internal carotid artery (ICA)–ophthalmic artery; 8, ICA–posterior communicating artery; 9, ICA bifurcation; 10, other area of ICA; 11, vertebral artery; 12, basilar artery; and 13, distal artery of posterior circulation.

After independent assessment of all the images, the DSA studies that caused interpretation disagreement between 2 readers were reviewed jointly for a final consensus interpretation. If multiple aneurysms were found on DSA in cases of acute subarachnoid hemorrhage, the location of the ruptured aneurysm was confirmed by nonenhanced CT and DSA.

If an aneurysm was considered probably or definitely present, both dome and neck diameters were measured for each aneurysm and the N/D ratio was calculated on both MDCTA and DSA images. All measures were performed on the workstation with an electronic caliper after appropriate magnification; the aneurysm dome and neck dimensions were measured at a selected projection, which allowed the optimal demonstration of the neck of the aneurysm. Each aneurysm was assigned 1 of 3 categories on the basis of the value of N/D ratio on MDCTA images and on DSA images: 1, narrow (N/D ratio, $<1/3$); 2, intermediate (N/D ratio, 1/3–2/3); and 3, wide (N/D ratio, $>2/3$).

In 40 patients who underwent both VRT and automated segmentation algorithms, the readers assessed independently whether VRT images after automated segmentation actually provided any additional information on the evaluation of the aneurysm. The time (in minutes) required for the complete analysis of each case was recorded for each reader.

Statistical Analysis

For statistical analysis, 2×2 tables of the true-positive, false-positive, true-negative, and false-negative cases of cerebral aneurysms at MDCTA, by using consensus interpretations of DSA as the standard of reference, were constructed. For the purposes of positive and negative correlation, "probably present" or "definitely present" were considered positive for aneurysm; all others were considered negative for aneurysm. Sensitivity, specificity, and accuracy of MDCTA for detection of aneurysms were calculated on both per-aneurysm and per-patient basis. Lesions that were considered false-positive or false-negative findings at the blinded review of the MDCTA images were reassessed retrospectively by the same 2 radiologists with knowledge of the DSA findings, and a consensus judgment was made as to the cause of the false-positive or false-negative results.

Interobserver agreement between both readers was determined by calculating κ values (poor agreement, $\kappa = 0$; slight agreement, $\kappa = 0.01–0.20$; fair agreement, $\kappa = 0.21–0.40$; moderate agreement, $\kappa = 0.41–0.60$; good agreement, $\kappa = 0.61–0.80$; and excellent agreement, $\kappa = 0.81–1.00$).[16] The comparisons between characterization of aneurysms (N/D ratio, lobularity, and relationship with the adjacent arterial branch) demonstrated by MDCTA and DSA were tested for statistical significance by use of the χ^2 test. P values $<.05$ were considered to indicate a statistically significant difference. All statistical analyses were performed with commercially available software (SPSS 10.0 for Windows, SPSS, Chicago, Ill).

Results

The image quality of MDCT angiograms was rated as excellent in 80 (94%) patients by reader 1 and in 81 (95%) by reader 2. Readers 1 and 2 rated image quality as adequate for diagnosis in 5 (6%) and 4 (5%) of 85 patients, respectively. None of the CT images, however, were rated as inadequate for diagnosis. In addition, the mean time taken for MDCTA image interpretation was 6.9 minutes for reader 1 and 8.2 minutes for reader 2.

At DSA, a total of 93 aneurysms was present in 71 of the 85 patients involved in the study; 16 patients had 2 aneurysms each and 3 patients had 3 aneurysms each (Fig 1). In 14 of the 85 patients, no aneurysm was identified by using MDCTA and DSA, and the evaluations were considered as true-negative by MDCTA. All 14 patients also had negative findings at repeat DSA.

According to MDCTA measurements (2 independent measurements were averaged for each aneurysm), 27 (29%) of 93 aneurysms were <3 mm; 22 (24%), 3–5 mm; and 44 (47%),

Table 1: Characteristics of false-positive ($n = 2$) and false-negative ($n = 10$) evaluations

Location	Size (mm)	Reader	Confidence	Main Reason for Results
False-negative				
Supraclinoid ICA	1.5	1 and 2	2, 1	Very small, close proximity to bone
Supraclinoid ICA	1.8	1 and 2	3, 2	Very small, close proximity to bone
Supraclinoid ICA	1.8	2	2	Very small
PcomA	1.5	1 and 2	2, 2	Very small, prominent infundibulum
PcomA	2.1	1 and 2	3, 3	Very small, prominent infundibulum
PcomA	2.8	1	3	Prominent infundibulum
MCA bifurcation	2.5	1	2	Obscured by overlapping vessels
MCA bifurcation	2.8	2	3	Obscured by overlapping vessels
A1	2.8	1	1	Unusual location
Basilar tip	3.9	2	1	Atypical configuration, kissing aneurysm
False-positive				
PcomA	1.9	2	4	Prominent infundibulum
PcomA	1.5	1	4	Prominent infundibulum

Note:–ICA indicates internal carotid artery; PcomA, posterior communicating artery; MCA, middle cerebral artery; A1, first segment of anterior cerebral artery. Confidence score refers to a 5-point scale of reader certainty in identifying the presence or absence of the aneurysms (1 = definitely not present; 2 = probably not present; 3 = equivocal; 4 = probably present; 5 = definitely present).

Table 2: Diagnostic performance of MDCTA according to the size of the aneurysm by independent readings

Size of Aneurysm	Sensitivity (%)	Specificity (%)	Positive Predictive Value (%)	Negative Predictive Value (%)	Accuracy (%)
<3 mm					
MDCTA reader 1	74.1 (20/27)	93.3 (14/15)	95.2	66.7	81.0
MDCTA reader 2	77.8 (21/27)	93.3 (14/15)	95.5	70.0	83.3
3–5 mm					
MDCTA reader 1	100 (22/22)	100 (14/14)	100	100	100
MDCTA reader 2	95.5 (21/22)	100 (14/14)	100	93.3	97.2
>5 mm					
MDCTA reader 1	100 (44/44)	100 (14/14)	100	100	100
MDCTA reader 2	100 (44/44)	100 (14/14)	100	100	100

Note:–MDCTA indicates multidetector row CT angiography. Numbers in parentheses indicate numbers of aneurysms.

>5 mm. The smallest aneurysm identified by MDCTA was 1.6 mm, and the largest was 14.1 mm (mean size, 5.1 mm ± 2.6 mm). Of the 93 aneurysms, 38 (40.8%) were located at the anterior communicating artery; 23 (24.7%), at the posterior communicating artery; 15 (16.1%), at the MCA (bi-/trifurcation); 8 (8.6%), at posterior circulation (3 of the tip of the basilar artery, 3 of the posterior inferior cerebellar artery, 1 of the superior cerebellar artery, and 1 of the posterior cerebral artery); 7 (7.5%), at the ICA; and 2 (2.2%), at the ACA.

Of the 93 aneurysms in our study, 86 were identified correctly for each reader at blinded review of the MDCTA images. Both readers missed 7 aneurysms each; 4 aneurysms were missed by both readers. The aneurysms missed by both readers were located at the posterior communicating artery ($n = 2$) and at the supraclinoid portion of the ICA ($n = 2$). Another 6 aneurysms were missed by 1 reader: 2 at the bifurcation of the MCA, 1 at the posterior communicating artery, 1 at the A1 segment of the ACA, 1 at the ICA, and 1 at the basilar tip. When the 2 readers' mistakes were combined, all but 1 missed aneurysm was <3 mm in maximal dimension (range, 1.5–3.9 mm; mean, 2.3 mm ± 0.8). The only aneurysm of >3 mm that was missed by reader 2 was the so-called "kissing aneurysm." In this case, MDCTA was interpreted to have demonstrated a bilobed aneurysm of the superior cerebellar artery, whereas 2 separate single-lobed aneurysms of the superior cerebellar artery and the basilar tip were revealed at DSA. All of these aneurysms could be identified, however, when MDCTA images were reviewed retrospectively in conjunction with the DSA images. All missed aneurysms were in patients with multiple aneurysms in whom the ruptured aneurysm was correctly identified by both readers at the MDCTA reading (Fig 1). Thus, all aneurysms missed by at least 1 of the 2 readers in our study were incidental noncausative aneurysms, which were apparent on DSA. There were 2 false-positive findings in 2 patients at MDCTA. In these patients, a posterior communicating aneurysm was identified on MDCTA by 1 reader each, but with DSA, there were infundibular dilations at the origin of the posterior communicating artery. Details of all the false-negative and false-positive results of MDCTA are listed in Table 1.

Compared with DSA, the overall sensitivity, specificity, and accuracy of MDCTA on a per-aneurysm basis were 92.5%, 93.3%, and 92.6%, respectively, for both readers independently. However, the sensitivity, specificity, and accuracy values of 100% were achieved by both readers with MDCTA for detection of aneurysms on a per-patient basis. Sensitivity, specificity, positive and negative predictive values, and diagnostic accuracy were also calculated according to the size of the aneurysm. The sensitivity of MDCTA for aneurysms <3 mm was 74.1% for reader 1 and 77.8% for reader 2; for ≥3 mm, it was 100% and 98.5%, respectively (Table 2). There were 6 aneurysms that were <2 mm in our study, and 4 of these small aneurysms were not identified by at least 1 reader at initial interpretation of MDCTA images. There was excellent interobserver agreement between 2 independent MDCTA readers for detection of aneurysm ($\kappa = 0.822 \pm 0.097$).

Table 3: N/D ratios of aneurysms as measured with DSA and MDCTA

	Reader 1		Reader 2	
N/D Ratio	DSA	MDCTA	DSA	MDCTA
<1/3	23	20	22	20
1/3–2/3	50	51	49	49
>2/3	20	22	22	24
Total	93	93	93	93

Note:–N/D indicates neck-to-dome ratio; DSA, digital subtraction angiography; MDCTA, multidetector row CT angiography.

Two of 93 aneurysms were fusiform, and it was not possible to measure dimensions of the neck in these aneurysms. The N/D ratios of aneurysm were, therefore, measurable in 91 aneurysms. Although the N/D ratio of aneurysm at MDCTA was slightly higher compared with that measured at DSA (0.50 ± 0.18 versus 0.45 ± 0.19, respectively, for reader 1 and 0.54 ± 0.21 versus 0.48 ± 0.19, respectively, for reader 2), this trend did not reach statistical significance ($P = .056$ for reader 1 and $P = .066$ for reader 2, respectively). Moreover, readers 1 and 2 overestimated the N/D ratios of 4 and 3 aneurysms, respectively; the N/D ratios of 2 aneurysms were overestimated by both readers (Table 3). In all but 1 aneurysm, the N/D ratio was overestimated at MDCTA by 1 grade; in 1 aneurysm, the N/D ratio was overestimated by 2 grades by both readers (Fig 2). There was no case with underestimation at MDCTA.

In addition, MDCTA was accurate in delineating the number of aneurysm lobes present and the relationship of the aneurysm with the adjacent arterial branches. However, in 2 aneurysms in reader 1 and 3 aneurysms in reader 2, MDCTA images were interpreted to have demonstrated single-lobed aneurysms, but DSA and subsequently surgery demonstrated that they were multilobed. Arterial branches adjacent to the aneurysm neck or dome were unequivocally demonstrated by MDCTA. When compared with DSA, all 18 adjacent arterial branches were identified correctly by both readers on MDCTA images. The accuracy of MDCTA for aneurysm lobularity and adjacent branch was 97% and 100%, respectively.

In this study, MDCTA images were reconstructed by using combinations of VRT and automated segmentation algorithms for the analysis of MDCTA data in 40 patients with 44 aneurysms. In all patients, bone structures could be removed successfully from the images without deleting the image of the aneurysm or arterial segment. Readers 1 and 2 judged that VRT images after automated segmentation provided useful additional information in 7 (17.5%) and 9 (22.5%) of 40 patients, respectively (Fig 3). However, in the remaining patients, both readers were of the opinion that automated segmentation algorithm did not provide any additional information. Additional information provided by automated segmentation algorithm included better visualization of an aneurysm projecting inferiorly ($n = 4$ for reader 1 and $n = 5$ for reader 2) and better differentiation of small aneurysms from bone that were located near the bony structures at the skull base ($n = 3$ for reader 1 and $n = 4$ for reader 2).

Discussion

Recent studies with 4-channel MDCT scanners reported that the sensitivity of MDCTA in diagnosing intracranial aneurysms ranged from 85% to 96% and specificity, from 83% to 97%.[17-21] These studies also reported greater sensitivity, compared with the previous single-detector row CTA studies, for the detection of small aneurysms. However, these studies also reported that a number of small aneurysms could be missed even by MDCT. Dammert et al[17] reported MDCTA in 50 patients, achieving a detection rate of 83% for aneurysms of <4 mm. Teksam et al[18] investigated 100 patients with 113 aneurysms by using MDCTA and reported a sensitivity of 84% for aneurysms of <4 mm. In a study of 178 aneurysms reported by Kangasniemi et al,[19] only 4 of 11 cerebral aneurysms of <2 mm in diameter detected by DSA were found by using MDCTA.

More recently, the use of 16-channel MDCTA in the detection of intracranial aneurysm was reported by Tipper et al.[22] They investigated 57 patients with suspected intracranial aneurysms and detected 51 of 53 aneurysms, with an overall sensitivity of 96% and specificity of 100%. They also found sensitivities of 91.7% for 2 independent readers for the detection of 12 aneurysms of <3 mm, with an interactive VRT algorithm.

The sensitivity rate of our study group was in accordance with the results of most previous MDCTA studies. However, the results of this study with a relatively large number of patients and aneurysms are poorer than those reported in a recent study by using 16-channel MDCT.[22] This result might be due to our aneurysm size; there were considerable differences in the aneurysm size between the 2 studies (mean diameter, 5.1 mm versus 6.3 mm; number of aneurysms of <3 mm, 27 versus 12; number of aneurysms of <2 mm, 6 versus 3). On the other hand, all missed aneurysms in our study could be identified at retrospective review in conjunction with the DSA images. This trial started immediately after the introduction of MDCT at our hospital. Therefore, we expected to reduce perceptive errors in the interpretation of MDCTA studies for intracranial aneurysms, with increasing reader experience.

In this study, false-negative results in 3 cases and false-positive results in 2 cases were related to the posterior communicating artery. These results are in agreement with those of previous reports, which had relatively poor sensitivities and specificities for the detection of posterior communicating arterial aneurysms.[11,13] That was mainly due to their small size (<3 mm) and similar morphologic features with infundibular dilations, which made their discrimination difficult. An "infundibulum" could be defined as a pyramidal dilation at the origin of a vessel with an artery arising from the apex. As seen in 5 false-negative or positive lesions in our study, however, it is difficult to distinguish a small posterior communicating artery aneurysm from an infundibular dilation. In addition, MDCTA may occasionally fail to reveal the tiny vessel that emerges from the top of an infundibular dilation, giving the false impression of a posterior communicating artery aneurysm. Therefore, we believe that considerable caution is required in the interpretation of small aneurysms (<3 mm) arising from the posterior communicating artery at MDCTA, particularly if observer confidence is low.

All missed aneurysms in our series were small unruptured aneurysms, which were found in patients with multiple aneurysms in whom the ruptured aneurysm was detected by MDCTA. These small noncausative aneurysms are considered generally unimportant in the acute setting because most of

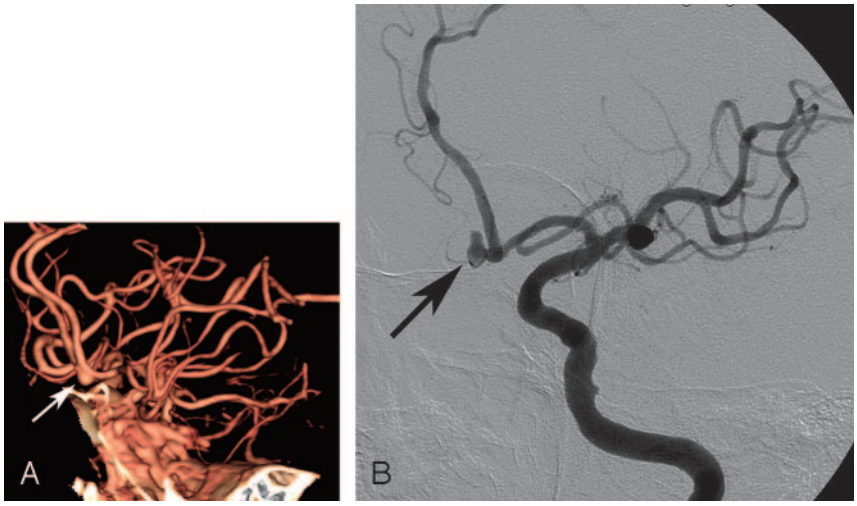

Fig 2. A 71-year-old woman with subarachnoid hemorrhage.

A, Left anterior oblique projection volume-rendered MDCTA image shows a saccular aneurysm arising from the anterior communicating artery (*arrow*). The neck of aneurysm was graded as wide (grade 3; N/D ratio, >2/3) by both readers on the basis of volume-rendered images.

B, DSA image of the left internal carotid artery, obtained in a projection similar to that of the DSA image shown in *A*, shows the narrow (grade 1; N/D ratio, <1/3) neck of the aneurysm (*arrow*).

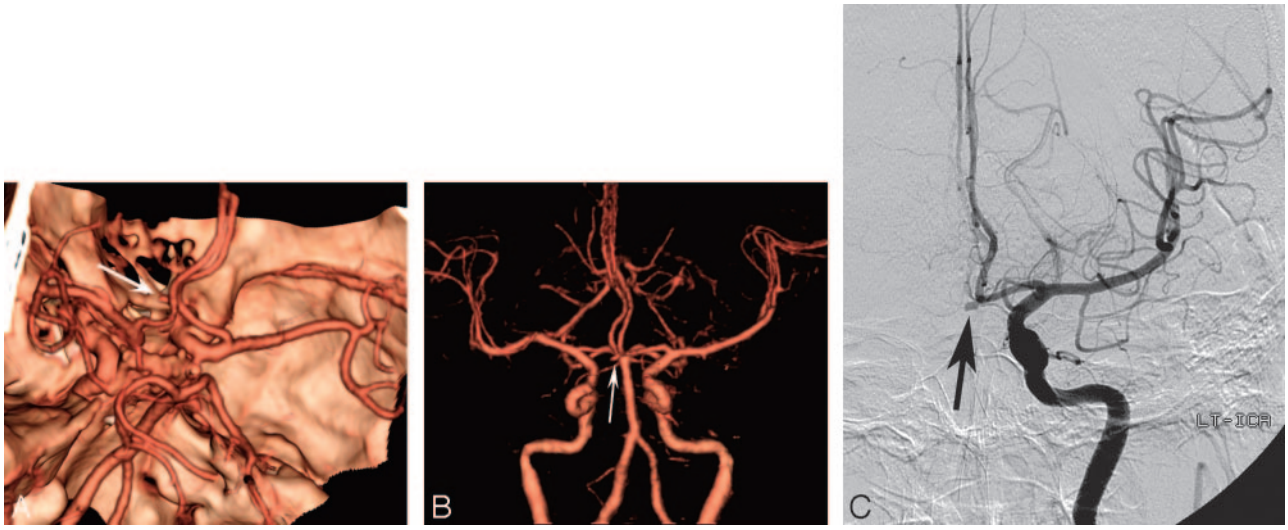

Fig 3. A 57-year-old man with subarachnoid hemorrhage.

A, Superior projection volume-rendered MDCTA image shows a small aneurysm of the anterior communicating artery (*arrow*). With this technique, the neck of the aneurysm is obscured by both overlying anterior cerebral arteries despite multiple projections (not shown).

B, Anteroposterior projection volume-rendered MDCTA image with automated segmentation shows laterally and inferiorly directed saccular aneurysm at the anterior communicating artery (*arrow*). The relations of the aneurysmal neck can be demonstrated better with this postprocessing software.

C, Corresponding DSA image of the left internal carotid artery shows the same aneurysm (*arrow*).

them do not require immediate treatment. Although the risk of rupture from small aneurysm is believed to be low,[23] we think that a complementary DSA should be considered if findings at MDCTA are equivocal.

In this study, accurate measurement of aneurysm dimension was not possible at DSA because the magnification factor was not calculated. On the other hand, MDCTA enabled digital measurements of aneurysm dimensions in any chosen plane, by using the CT software calipers. Therefore, we compared the N/D ratios of aneurysms by MDCTA and DSA, instead of by aneurysm dome and neck dimensions. We found a tendency with MDCTA to overestimate the N/D ratios compared with those obtained with DSA, though the difference was not significant. These results are in agreement with a previous report published by Wintermark et al.[21] N/D ratio of aneurysm is important because it may affect the selection of the treatment options.[24] In a few patients in our series, there was considerable overestimation of the N/D ratio of aneurysms, which may have led to possible therapeutic option changes. In such cases, additional processing with the use of a virtual endoscopic image may reduce potential errors in the measurement of N/D ratio.

Our results also suggest that MDCTA can provide valuable information concerning the lobularity and the relationship with adjacent branches. MDCTA still does not have as much spatial resolution as DSA; the distal part of adjacent branches in a few patients in our series was not visualized. However, the origin of adjacent branches was well demonstrated in all patients. These MDCTA capabilities for accurate aneurysm characterization (ie, N/D ratio, lobularity, and the presence of adjacent arterial branches) were deemed helpful in making a therapeutic decision concerning whether to use surgical clipping or endovascular treatment.

With the introduction of MDCT scanners, there has been increased demand and use with regard to vascular applications.[25] Fundamental theoretic advantages of MDCT include

substantially faster scanning speed, greater volumetric coverage, and higher longitudinal spatial resolution than was possible with single-detector row CT scanners.[15] These technical advances are reflected in the overall image quality of our MDCTA studies, in which all examinations were assessed as adequate (grade 2) to excellent (grade 3) by both readers. Image quality was rated as adequate in 5 patients by reader 1 and in 4 by reader 2. The reduced image quality in these patients was caused by the presence of venous enhancement and patient motion artifacts; however, the presence of venous contamination and artifacts did not affect aneurysm evaluation for diagnostic purposes.

Recently upgraded software of the workstation that allows automated segmentation of bony structures was available in 40 cases of our study group. This advanced postprocessing software can reduce the time required for 3D reconstructions of CT angiographic data and avoid overlapping bone in a fully automatic way. This software appeared of particular value for the detection and characterization of aneurysms projecting inferiorly and lying in areas near bony structures.

In current publications that deal with MDCTA, most authors used combinations of VRT, maximum intensity projection (MIP), and multiplanar reconstruction for the analysis of MDCTA axial data. The MIP method has an advantage over VRT for differentiating parietal calcification and intraluminal thrombus from true vascular lumen.[26] However, calcification at the wall or thrombus within the lumen of an aneurysm can be clearly shown on the careful review of the source images. Neither mural calcification nor intraluminal thrombus was detected in any case of aneurysm in our series on the basis of source data. Furthermore, the MIP technique has a particular disadvantage because it requires the long postprocessing time and operator's extensive experience for adequate removal of the cranial bones.[27] The bones at the base of the skull may be quite difficult to remove, considering the large amount of transverse images associated with MDCT. Therefore, we used the VRT method instead of the MIP algorithm for the comparison with DSA in this study. The VRT method is, in our experience, far quicker and easier to produce than MIP algorithms and can give better anatomic detail of the intracranial vasculature. The 4D Angio software package (Rapidia 3D) allows rapid VRT images to be produced, which highlight the vessels over the bony landmarks.

In this study, all 3D image postprocessing was routinely performed by skilled technicians without direct neuroradiologist supervision. To reduce reconstruction time, we also used a fixed number of standard viewing projections, even if free rotation of the reformatted images was possible during image interpretation. In most patients of this series, experienced technicians were able to generate the standardized VRT images in less than 8 minutes, which was shorter than that reported in previous studies.

The results of this study suggest that MDCTA is equally as sensitive as DSA in the detection of intracranial aneurysms of >3 mm. It also exhibits 100% detection rate for ruptured aneurysms. We also showed that MDCTA is capable of accuracy in aneurysm characterization and that image acquisition and processing can be performed rapidly. Therefore, MDCTA clearly has a role in the rapid evaluation of patients with acute subarachnoid hemorrhage. It seems likely that treatment decisions can be made on the basis of MDCTA alone in emergency situations. As such, we believe that current MDCTA may replace diagnostic DSA for the initial management in a substantial proportion of patients with aneurysmal subarachnoid hemorrhage. It is expected that further technical advances with MDCT offering 64 or more detector rows and upgraded postprocessing software will improve the sensitivity and specificity of MDCTA.

We acknowledge several limitations of our study. A major limitation was the relatively high prevalence of aneurysm (84%) in our study population, which might have introduced observer expectation bias. There has been evidence that increased disease prevalence could have led to an apparent improvement in the sensitivity and specificity of a diagnostic examination.[28] Furthermore, subarachnoid hemorrhage in our population may provide a strong clue to the presence and/or site of an aneurysm; a reader might be more confident about an equivocal finding. Another possible problem in our study relates to the fact that we used only VRT algorithms to reconstruct 3D images of the aneurysm. Further studies are needed to compare the diagnostic value of different reconstruction techniques, including MIP and VRT, for analysis of the MDCT angiograms.

Finally, we used DSA as the standard of reference for imaging cerebral aneurysms; small aneurysms, however, could not be depicted with this technique. Recently, 3D rotational DSA has been developed and used clinically, but its high price prevents it from being used in many centers.[29-30] 3D rotational DSA enables us to obtain accurate information regarding the cerebral aneurysms and adjacent branches, providing visualization of them from different perspectives without vessel overlap.[31] Recent studies have shown that 3D DSA can depict more intracranial aneurysms and provide better anatomic details important for the therapeutic planning than conventional DSA can.[31-32]

In conclusion, MDCTA is an accurate imaging technique for detection and characterization of intracranial aneurysms and has the potential to substitute, in most cases, for DSA. However, MDCTA still has limited sensitivity in detecting aneurysms of <3 mm, despite its technical advances.

References

1. King JT Jr. **Epidemiology of aneurysmal subarachnoid hemorrhage.** *Neuroimaging Clin N Am* 1997;7:659–68
2. Cloft HJ, Joseph GJ, Dion JE. **Risk of cerebral angiography in patients with subarachnoid hemorrhage, cerebral aneurysm, and arteriovenous malformation: a meta-analysis.** *Stroke* 1999;30:317–20
3. Hankey GJ, Wrlow CP, Sellar RJ. **Cerebral angiographic risk in mild cerebrovascular disease.** *Stroke* 1990;21:209–22
4. Ronkainen A, Puranen M, Hernesniemi JA, et al. **Intracranial aneurysms: MR angiographic screening in 400 asymptomatic individuals with increased familial risk.** *Radiology* 1995;195:35–40
5. Wiebers DO, Torres VE. **Screening for unruptured intracranial aneurysms in autosomal-dominant polycystic kidney disease.** *N Engl J Med* 1992;327:953–55
6. Aoki S, Sasaki Y, Machida T, et al. **Cerebral aneurysms: detection and delineation using 3-D-CT angiography.** *AJNR Am J Neuroradiol* 1992;13:1115–20
7. Dillon EH, Van Leeuwen MS, Fernandez MA, et al. **Spiral CT angiography.** *AJR Am J Roentgenol* 1993;160:1273–78
8. Ogawa T, Okudera T, Noguchi K, et al. **Cerebral aneurysms: evaluation with three dimensional CT angiography.** *AJNR Am J Neuroradiol* 1996;17:447–54
9. Preda L, Gaetani P, Rodriguez V, et al. **Spiral CT angiography and surgical correlations in the evaluation of intracranial aneurysms**. *Eur Radiol* 1998;8:739–45
10. Alberico RA, Patel M, Casey S, et al. **Evaluation of the circle of Willis with**

three-dimensional CT angiography in patients with suspected intracranial aneurysms. *AJNR Am J Neuroradiol* 1995;16:1571–80
11. Anderson GB, Steinke DE, Petruk KC, et al. **Computed tomographic angiography versus digital subtraction angiography for the diagnosis and early treatment of ruptured intracranial aneurysms.** *Neurosurgery* 1999;45:1315–20
12. Korogi Y, Takahashi M, Katada K, et al. **Intracranial aneurysms: detection with three-dimensional CT angiography with volume rendering—comparison with conventional angiographic and surgical findings.** *Radiology* 1999;211: 497–506
13. Velthuis BK, Van Leeuwen MS, Witkamp TD, et al. **Computerized tomography angiography in patients with subarachnoid hemorrhage: from aneurysm detection to treatment without conventional angiography.** *J Neurosurg* 1999;91: 761–67
14. White PM, Teasdale EM, Wardlaw JM, et al.. **Intracranial aneurysms: CT angiography and MR angiography for detection—prospective blinded comparison in a large patient cohort.** *Radiology* 2001;219:739–49
15. Kato Y, Nair S, Sano H, et al. **Multi-slice 3D-CTA: an improvement over single slice helical CTA for cerebral aneurysms.** *Acta Neurochir (Wien)* 2002;144: 715–22
16. Landis JR, Koch GG. **An application of hierarchical kappa-type statistics in the assessment of majority agreement among multiple observers.** *Biometrics* 1977; 33:363–74
17. Dammert S, Krings T, Moller-Hartmann W, et al. **Detection of intracranial aneurysms with multislice CT: comparison with conventional angiography.** *Neuroradiology* 2004;46:427–34
18. Teksam M, McKinney A, Casey S, et al. **Multi-section CT angiography for detection of cerebral aneurysms.** *AJNR Am J Neuroradiol* 2004;25:1485–92
19. Kangasniemi M, Makela T, Koskinen S, et al. **Detection of intracranial aneurysms with two-dimensional and three-dimensional multislice helical computed tomographic angiography.** *Neurosurgery* 2004;54:336–40
20. Jayaraman MV, Mayo-Smith WW, Tung GA, et al. **Detection of intracranial aneurysms: multi-detector row CT angiography compared with DSA.** *Radiology* 2004;230:510–18
21. Wintermark M, Uske A, Chalaron M, et al. **Multislice computerized tomography angiography in the evaluation of intracranial aneurysms: a comparison with intraarterial digital subtraction angiography.** *J Neurosurg* 2003;98: 828–36
22. Tipper G, U-King-Im JM, Price SJ, et al. **Detection and evaluation of intracranial aneurysms with 16-row multislice CT angiography.** *Clin Radiol* 2005;60: 565–72
23. Cromptom M. **Mechanisms of growth and rupture in cerebral berry aneurysms.** *BMJ* 1996;1:1138–42
24. Fernadez Zubillaga A, Guglielmi G, Vinuela F, et al. **Endovascular occlusion of intracranial aneurysms with electrically detachable coils: correlation of aneurysm neck size and treatment results.** *AJNR Am J Neuroradiol* 1994;15:815–20
25. Rubin GD, Shiau MC, Leung AN, et al. **Aorta and iliac arteries: single versus multiple detector-row helical CT angiography.** *Radiology* 2000;215:670–76
26. Ng S, Wong H, Ko S, et al. **CT angiography of intracranial aneurysms: advantages and pitfalls.** *Eur J Radiol* 1997;25:14–19
27. Johnson PT, Halpern EJ, Kuszyk BS, et al. **Renal artery stenosis: CT angiography-comparison of real-time volume-rendering and maximum intensity projection algorithms.** *Radiology* 1999;211:337–43
28. Brenner H, Gefeller O. **Variation of sensitivity, specificity, likelihood ratios and predictive values with disease prevalence.** *Stat Med* 1997;16:981–91
29. Sugahara T, Korogi Y, Nakashima K, et al. **Comparison of 2D and 3D digital subtraction angiography in evaluation of intracranial aneurysms.** *AJNR Am J Neuroradiol* 2002;23:1545–52
30. Bidaut LM, Laurent C, Piotin M, et al. **Second-generation three-dimensional reconstruction for rotational three-dimensional angiography.** *Acad Radiol* 1998;5:836–49
31. Tanoue S, Kiyosue H, Kenai H, et al. **Three-dimensional reconstructed images after rotational angiography in the evaluation of intracranial aneurysms: surgical correlation.** *Neurosurgery* 2000;47:866–71
32. Hochmuth A, Spetzger U, Schumacher M. **Comparison of three dimensional rotational angiography with digital subtraction angiography in the assessment of ruptured cerebral aneurysms.** *AJNR Am J Neuroradiol* 2002;23:1199–205